Constructing a Virtual Large Reference Plate with High-precision for Calibrating Cameras with Large FOV

LIU Dong, ZHANG Rui*, ZHANG Jin, LI Weishi

(*Anhui Province Key Laboratory of Measuring Theory and Precision Instrument, School of Instrument Science and Opto-Electronics Engineering, Hefei University of Technology, Hefei 230009*)

Abstract: It is well known that the accuracy of camera calibration is constrained by the size of the reference plate, it is difficult to fabricate large reference plates with high precision. Therefore, it is non-trivial to calibrate a camera with large field of view (FOV). In this paper, a method is proposed to construct a virtual large reference plate with high precision. Firstly, a high precision datum plane is constructed with a laser interferometer and one-dimensional air guideway, and then the reference plate is positioned at different locations and orientations in the FOV of the camera. The feature points of reference plate are projected to the datum plane to obtain a virtual large reference plate with high-precision. The camera is moved to several positions to get different virtual reference plates, and the camera is calibrated with the virtual reference plates. The experimental results show that the mean re-projection error of the camera calibrated with the proposed method is 0.062 pixels. The length of a scale bar with standard length of 959.778mm was measured with a vision system composed of two calibrated cameras, and the length measurement error is 0.389mm.

Keywords: Camera Calibration, Large Flied of View, Laser Interferometer, Virtual Reference Plate

1 Introduction

In recent years, the appliction of various vision systems in measuring large-scale and complex parts in aerospace, automobile manufacturing and etc. pose a challenge to the calibration accuracy of the camera with large field of view[1-3]. as the measurement accuracy of the vision system is dependent on the calibration accuracy of the camera parameters. Zhang's method of camera calibration[4], which is widely used in practice, is based on a reference plate with certain features. The proportion of the plate in the image plane of the camera has an important effect on the accuracy of camera calibration. However, the size of the commonly used reference plate, such as checkerboard, is limited by the manufacturing technology and cost, and it is difficult to calibrate a camera large FOV accurately with a small reference plate.

Several methods have been proposed to construct a virtual large reference artifact to calibrate the camera with large FOV. Liu et al.[5-7] used a CMM to move circular LED markers or infrared LED markers uniformly in 3D space and construct a virtual large 3D artifacts. The size of the virtual 3D artifact is limited by the measuring range of the CMM, and in order to ensure the accuracy of the artifact, a large number of different markers are required to be distributed in each position in space. Yang[8] proposed to project a laser

line on a real plane to construct a virtual large plate. Apparently, the accuracy is dependent on the planeness error of the real plane and the size of the laser spot. Sun et al.[9] proposed a method to construct a 3D virtual artifact using a small reference plate. However, it is difficult to measure the the relative position between different plates accurately, and we can not guarantee the accuracy of the virtual artifact as a result.

Several methods have also been proposed to construct a virtual large reference plate using a small reference plate. Zhang et al.[10] proposed to use a laser tracker to measure the transformation of a small reference plate in 3-Dimensional (3D) space and construct a virtual large reference plate. However, it is difficult to fix the small reference plate in 3D space and measure it precisely. Yu et al.[11] projected multiple images of a small reference plate onto a one reference plane to construct a large virtual plate. However, it is non-trivial to compute the transformation matrix between two distroted images of the reference plate accurately.

In this paper, we propose a method to constructing a virtual large reference plate with high-accuracy, and we show that we can calibrate the camera with large FOV precisely.

2 Camera Model

Without loss of generality, based on the pinhole camera model, the homogeneous coordinates of a 3D point M in the world coordinate system are denoted as $M=(X_w, Y_w, 0, 1)$, the homogeneous coordinate of the point in the pixel coordinate system of camera is $m=(u, v, 1)$. The relationship between M and the corresponding point m in the pixel coordinate system is given in Eq. (1) .

$$s\begin{bmatrix} u \\ v \\ 1 \end{bmatrix} = \boldsymbol{A}\begin{bmatrix} \boldsymbol{r}_1 & \boldsymbol{r}_2 & \boldsymbol{r}_3 & \boldsymbol{t} \end{bmatrix}\begin{bmatrix} X_w \\ Y_w \\ Z_w \\ 1 \end{bmatrix} \tag{1}$$

where s is the scale factor, $\boldsymbol{r}_i$ is the ith column of the $\boldsymbol{R}$, $[\boldsymbol{R} \quad \boldsymbol{t}]$ is the extrinsic parameter matrix of the camera, including the rotation matrix and translation matrix corresponding to the world coordinate system and the camera coordinate system. Because of $Z_w=0$, Eq. (1) can be rewritten as:

$$\begin{bmatrix} u \\ v \\ 1 \end{bmatrix} = \frac{1}{s}\boldsymbol{A}\begin{bmatrix} \boldsymbol{r}_1 & \boldsymbol{r}_2 & \boldsymbol{t} \end{bmatrix}\begin{bmatrix} X_w \\ Y_w \\ 1 \end{bmatrix} \tag{2}$$

and $\boldsymbol{A}$ is the intrinsic parameter matrix of the camera, which is given by Eq. (3) :

$$\boldsymbol{A} = \begin{bmatrix} \alpha & \gamma & u_0 \\ 0 & \beta & v_0 \\ 0 & 0 & 1 \end{bmatrix} \tag{3}$$

Where (u_0,v_0) are the coordinates of the principal point, α and β are the scale factors in u and v axes of the image, respectively, and γ is the parameter describing the skew of the two image axes. The homography matrix $\boldsymbol{H}$ reflects the corresponding position relationship between a point on a plane of space and its imaging point on the camera imaging plane, so it can be obtained:

$$\begin{bmatrix} \boldsymbol{h}_1 & \boldsymbol{h}_2 & \boldsymbol{h}_3 \end{bmatrix} = \frac{1}{s}\boldsymbol{A}\begin{bmatrix} \boldsymbol{r}_1 & \boldsymbol{r}_2 & \boldsymbol{t} \end{bmatrix} \tag{4}$$

$\boldsymbol{h}_i$ are used to represent the i column of matrix $\boldsymbol{H}$.

In applications, the camera lens is distorted because of the manufacturing error, this will cause the actual image points to deviate from the theoretical image points. The radial distortion and tangential distortion of camera lens have significant influence on the measurement accuracy of visual measurement[12], so only these two kinds of distortions will be considered in this paper. $m_d=(x_d, y_d, 1)$ represents the actual image point of M, $m=(x, y, 1)$ represents the theoretical image point of M, Then the camera distortion can be expressed as:

$$\begin{aligned} x_d &= x(1+k_1r^2+k_2r^4)+[2p_1y+p_2(r^2+2x^2)] \\ y_d &= v(1+k_1r^2+k_2r^4)+[2p_2x+p_1(r^2+2y^2)] \end{aligned} \tag{5}$$

where $r=\sqrt{x^2+y^2}$, k_1 and k_2 are the radial distortion coefficients of the camera, while p_1 and p_2 are the tangential distortion coefficients.

3 View of the Method

In this paper, the images of a small reference plate at multiple locations are projected onto one datum plane to construct a virtual large reference plate. Firstly,

a datumn plane is constructed. Then, the virtual points on the datumn plane corresponding to the feature points on each image of the small reference plate are computed. Finally, the images of the small reference plate in multiple positions are integrated into a large virtual reference plate.

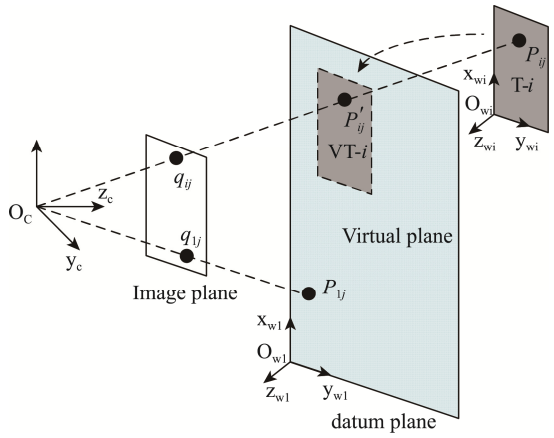

Fig.1 Schematic Diagram of Constructing a Virtual Plate

As shown in Fig.1, T-i is the ith position of the small reference plate, P_{ij} represents the jth feature point on the ith position, and the corresponding image point on the camera imaging plane is q_{ij}. According to projective geometry, there must be a point $P_{ij}^{'}$ on the virtual datum, its corresponding image point is q_{ij}, i.e. $P_{ij}^{'}$ is the projection point of the P_{ij} on the datum plane.

The accuracy of computing the coordinates of a virtual projection points on the datum plane is dependent on the accuracy of the transformation matrix between the datum plane and the camera imaging plane. In comparison with the method proposed in Ref. [11], we proposed a more accurate method to construct the datum plane.

4 Constructing the Virtual Large Reference Plate

4.1 Construction of Large Size Virtual Datum Plane

In this paper, a high-precision 1-dimensional guide rail is used to move a checkerboard to several position and obtain the corresponding images, respectively. to the images are used to construct a datum plane. As shown in Fig.2, position 1 is the initial position of the checkerboard, and we move the checkerboard to several positions, and the translation distance of the small target is measured with a laser interferometer.

We can not guarantee that the checkerboard at different positions is on the same plane. However, a column of the corner points at each position can be guaranteed to be on the same plane. Therefore, only the first column of checkerboard corner points at each position are selected to construct the datum plane.

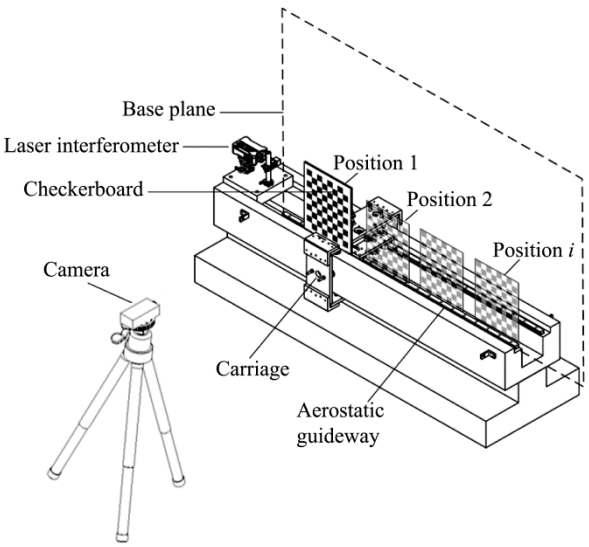

Fig.2 Schematic Diagram of Constructing the Datum Plane

The position relationship of different feature points on the plane can be computed as follows. Denote the homography corresponding to the checkerboard at the ith position as $\boldsymbol{H}^{(i)}$, and $\boldsymbol{h}_i$ and $\boldsymbol{r}_i$ represent the i column of $\boldsymbol{H}$ matrix and $\boldsymbol{R}$ matrix, respectively. According to the camera model given in Section 2, $\boldsymbol{R}$ matrix is orthonormal. We can get:

$$\boldsymbol{h}_1^T \boldsymbol{A}^{-T} \boldsymbol{A}^{-1} \boldsymbol{h}_2 = 0 \tag{6}$$

$$\boldsymbol{h}_1^T \boldsymbol{A}^{-T} \boldsymbol{A}^{-1} \boldsymbol{h}_1 = 1 \tag{7}$$

$$\boldsymbol{h}_2^T \boldsymbol{A}^{-T} \boldsymbol{A}^{-1} \boldsymbol{h}_2 = 1 \tag{8}$$

Let $\boldsymbol{B}=\boldsymbol{A}^{-T}\boldsymbol{A}^{-1}$, we can get:

$$\boldsymbol{h}_1^{(1)T}\boldsymbol{B}\boldsymbol{h}_2^{(1)}=0 \tag{9}$$

$$\boldsymbol{h}_1^{(1)T}\boldsymbol{B}\boldsymbol{h}_1^{(1)}=1 \tag{10}$$

$$\boldsymbol{h}_2^{(1)T}\boldsymbol{B}\boldsymbol{h}_2^{(1)}=1 \tag{11}$$

When the checkerboard is located at position 1, there are three constraints on the camera parameters. According to Eq.(4), the translation relationship between the first position and the second position is:

$$(\boldsymbol{t}^{(2)}-\boldsymbol{t}^{(1)})=\boldsymbol{A}^{-1}\left(\frac{\boldsymbol{h}_3^{(2)}}{\lambda^{(2)}}-\frac{\boldsymbol{h}_3^{(1)}}{\lambda^{(1)}}\right)=a\boldsymbol{R}v \tag{12}$$

where $\lambda^{(i)}=1/s^{(i)}$, $\boldsymbol{R}$ is the rotation matrix, $\boldsymbol{v}$ is the movement direction of the guideway in the world coordinate system, and a is the translation distance between the first position and the ith position. The Frobenius norm of the translation between the first position and the i position can be expressed as:

$$\begin{aligned}&(\boldsymbol{t}^{(i)}-\boldsymbol{t}^{(1)})\boldsymbol{T}(\boldsymbol{t}^{(i)}-\boldsymbol{t}^{(1)})\\&=\left(\frac{\boldsymbol{h}_3^{(i)}}{\lambda^{(i)}}-\frac{\boldsymbol{h}_3^{(1)}}{\lambda^{(1)}}\right)^T\boldsymbol{A}^{-T}\boldsymbol{A}^{-1}\left(\frac{\boldsymbol{h}_3^{(i)}}{\lambda^{(i)}}-\frac{\boldsymbol{h}_3^{(1)}}{\lambda^{(1)}}\right)\\&=a^2\boldsymbol{v}^T\boldsymbol{R}^T\boldsymbol{R}\boldsymbol{v}=a^2\end{aligned} \tag{13}$$

Multiply both sides of Eq. 9 by $(\lambda^{(1)})^2$, we get:

$$\begin{aligned}&\left(\frac{\lambda^{(1)}}{\lambda^{(i)}}\boldsymbol{h}_3^{(i)}-\boldsymbol{h}_3^{(1)}\right)^T\boldsymbol{A}^{-T}\boldsymbol{A}^{-1}\left(\frac{\lambda^{(1)}}{\lambda^{(i)}}\boldsymbol{h}_3^{(i)}-\boldsymbol{h}_3^{(1)}\right)\\&=a^2\lambda^{(1)}\lambda^{(1)}\end{aligned} \tag{14}$$

The rotation matrix $\boldsymbol{R}$ does not change during the translation process, so

$$\boldsymbol{r}_1=\frac{\boldsymbol{A}^{-1}}{\lambda^{(1)}}\boldsymbol{h}_1^{(1)}=\frac{\boldsymbol{A}^{-1}}{\lambda^{(i)}}\boldsymbol{h}_1^{(i)} \tag{15}$$

Since the rank of m atrix $\boldsymbol{A}^{-1}$ is 3, we can obtain:

$$\frac{\lambda^{(1)}}{\lambda^{(i)}}=\frac{\boldsymbol{h}_1^{(1)}}{\boldsymbol{h}_1^{(i)}}=\frac{\left|\boldsymbol{h}_1^{(1)}\right|}{\left|\boldsymbol{h}_1^{(i)}\right|} \tag{16}$$

Therefore, Eq. (14) can be formulated as:

$$\begin{aligned}&\left(\frac{\left|\boldsymbol{h}_1^{(1)}\right|}{\left|\boldsymbol{h}_1^{(i)}\right|}\boldsymbol{h}_3^{(i)}-\boldsymbol{h}_3^{(1)}\right)^T\boldsymbol{B}\left(\frac{\left|\boldsymbol{h}_1^{(1)}\right|}{\left|\boldsymbol{h}_1^{(i)}\right|}\boldsymbol{h}_3^{(i)}-\boldsymbol{h}_3^{(1)}\right)\\&=a^2\left(\boldsymbol{h}_1^{(1)}\right)^T\boldsymbol{B}\boldsymbol{h}_1^{(1)}\end{aligned} \tag{17}$$

Three constraints have been provided for solving the internal parameters of the camera in Eq.(9)- Eq.(11). Eq.(17) provides the fourth constraint. Since the first and second column vectors of $\boldsymbol{H}^{(1)}$ are parallel to the first and second column vectors of $\boldsymbol{H}^{(2)}$, and the scaling factors $\lambda^{(1)}$ and $\lambda^{(i)}$ are unknown respectively, there are 11 unknown different elements in $\boldsymbol{H}^{(1)}$ and $\boldsymbol{H}^{(2)}$. The camera has 6 degrees-of-freedom (DOF), and there are 11–6=5 unkown parameters. When γ=0, the initial values of the camera parameters can be solved under the condition that the translation direction is unknown but the length is known. Once the initial value of A is known, the extrinsic parameters of each image can be calculated according to Zhang's method, and the position relationship between the checkerboard feature points at each position can be further solved to obtain the datum plane.

4.2 Computing the Coordinates of Virtual Feature Points

In Fig.1, the homogeneous coordinates of a feature points on the datum plane are $P_{1j}=(x_{w1j}, y_{w1j}, 0, 1)$, and the corresponding image homogeneous coordinates of are $q_{1j}=(u_{1j}, v_{1j}, 1)$. The homogeneous coordinates of a feature points on the T-2 plane are $P_{2j}=(x_{w2j}, y_{w2j}, 0, 1)$, and the corresponding image homogeneous coordinates are $q_{2j}=(u_{2j}, v_{2j}, 1)$. Then, according to Eq.(1) :

$$q_{1j}=\lambda_1\boldsymbol{A}\begin{bmatrix}\boldsymbol{R}_1 & \boldsymbol{t}_1\end{bmatrix}P_{1j} \tag{18}$$

$$q_{2j}=\lambda_2\boldsymbol{A}\begin{bmatrix}\boldsymbol{R}_2 & \boldsymbol{t}_2\end{bmatrix}P_{2j} \tag{19}$$

Obviously there is a point $P_{2j}^{'}=(x_{w2j}^{'}, y_{w2j}^{'}, 0, 1)$ in datum plane whose image is also q_{2j}, i.e.

$$q_{2j}=\lambda_2\boldsymbol{A}\begin{bmatrix}\boldsymbol{R}_2 & \boldsymbol{t}_2\end{bmatrix}P_{2j}^{'} \tag{20}$$

So $P_{2j}^{'}$ is the projection of P_{2j} onto T-1 plane. Let $\boldsymbol{H}_i=s_i\boldsymbol{A}[\boldsymbol{R}_i \quad \boldsymbol{t}_i]$, we can deduce the following from Eq. (18) - (20).

$$\begin{bmatrix}x_{w2j}'\\y_{w2j}'\\1\end{bmatrix}=\boldsymbol{H}_1^{-1}\cdot\boldsymbol{H}_2\cdot\begin{bmatrix}x_{w2j}\\y_{w2j}\\1\end{bmatrix} \tag{21}$$

According to Eq.(21), all feature points on T-2 plane can be projected on the datum plane. Similarly, the feature points on other positions of the small checkerboard can be projected on the datum plane, and we get a virtual large reference plate for camera calibration.

5 Camera Calibration

Due to the small occupation ratio of the checkerboard in the image, the errors in solving $\boldsymbol{H}_i$ are non-neglible, and the intrinsic parameters of the camera need to be further optimized.

Let P_{ijk} represent the coordinates of the jth feature point in O_w-$x_w y_w z_w$ coordinate system of the ith small target on the kth virtual large reference plate. The image coordinates of the theoretical imaging point q_{ijk} of P_{ijk} are different from the image coordinates of the actual imaging point $\tilde{q}_{ijk}$ as a result of the errors in solving $\boldsymbol{H}_i$. Therefore, we use the following function to optimize the intrinsic parameters of the camera.

$$f(w) = \min \sum_{k=1}^{m} \sum_{j=1}^{n} \sum_{i=1}^{l} \left| \tilde{q}_{ijk} - q_{ijk} \right|^2 \tag{22}$$

where w=($\mathbf{A}$, k_1, k_2, p_1, p_2, $\mathbf{R}_k$, $\mathbf{t}_k$, $\mathbf{H}_{ik}$). m is the number of virtual large reference, n is the number of feature points on the cherckerboard, and l is the number of positions of the cherckerboard used to construct the large virtual reference plate. The optimal solution of the function defined in Eq.(22) was solved using Levenberg-Marquart algorithm.

6 Experimental Verification

In order to verify the calibration performance of the proposed method, the method proposed in this paper was compared with the traditional calibration method with a small cherckerboard and a calibration method proposed in Ref. [11] under the same experimental conditions.

The camera to be calibrated is TS4MCL-180M industrial camera with the pixel size of 5.5μm×5.5μm, and the image resolution is 2048×2048. The checkerboard contains a pattern of 15×10 black and white grids, whose size is 200mm×200mm. The FOV of the camera was set to be 2m×2m, and the depth of view of the camera is 2.5m.

Firstly, according to Zhang's method, the checkerboard is used to calibrate the camera. During the calibration process, the checkerboard was moved several times to ensure that the checkerboard could cover the FOV as much as possible to calibrate the camera.

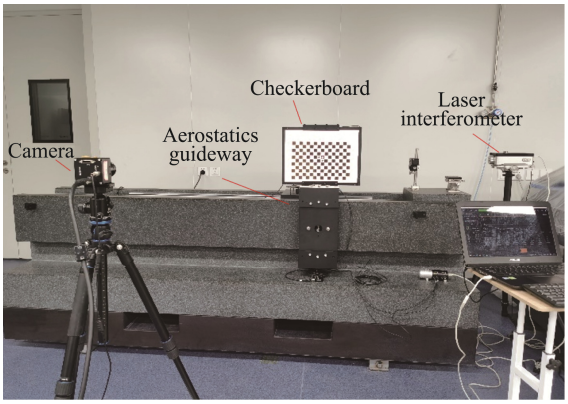

Fig.3 Experimental Device

Then, according to the method proposed in Ref. [11], the checkerboard was placed in several positions and poses in space to ensure that the checkerboard is distributed as evenly as possible in the FOV. The checkerboard plane at the first position was selected as the datum plane, and the checkerboards in other positions were projected onto the datum plane to obtain a virtual reference plate. The camera was moved and the above steps were repeated until sufficient virtual reference plates were obtained, and all virtual reference plates were used to calibrate.

Finally, the method proposed in this paper was used to calibrate the camera. The experimental equipment is shown in Fig.3. The checkerboard was fixed on an air bearing, high-precision guideway. The checkerboard was moved to several positions, and the displacement was measured using a laser interferometer and the datum plane was computed with the obtained images. Then, the checkerboard was placed in space to fill the entire FOV as much as possible, and a virtual reference plate was constructed. The camera was moved to different position and the above steps were repeated until sufficient virtual reference plates were obtained, and the obtained virtual reference plates were used for camera calibration.

The experiments were repeated for 10 times, and the mean reprojection error(MRE) of all corners of the checkerboard was calculated to evaluate the calibration accuracy. The results are given in Table 1.

Table 1 The Mean Reprojection Error

No.	Zhang's Method MRE/Pixel	Ref. [11] MRE/Pixel	The Proposed Method MRE/Pixel
1	0.077	0.076	0.067
2	0.084	0.077	0.063
3	0.082	0.077	0.065
4	0.087	0.075	0.058
5	0.073	0.072	0.061
6	0.088	0.071	0.062
7	0.074	0.073	0.064
8	0.084	0.076	0.059
9	0.073	0.074	0.061
10	0.077	0.073	0.057
Mean Value	0.080	0.074	0.062

According to Table 1, the mean reprojection error of the proposed method is 0.062 pixels, which is smaller than that of the two other methods.

In order to further verify the improvement of the calibration accuracy of the camera, two cameras were calibrated using the three methods, and a binocular vision system was built to measure the scale bar of the Creaform C-Track system as shown in Fig.4. There are eight reflective markers on the bar. The distance between each pair of markers shown in Fig.4 has been calibrated by Creaform, and is used as the reference value in this experiment. The calibrated distance and the corresponding measurement uncertainty are given in Table 2.

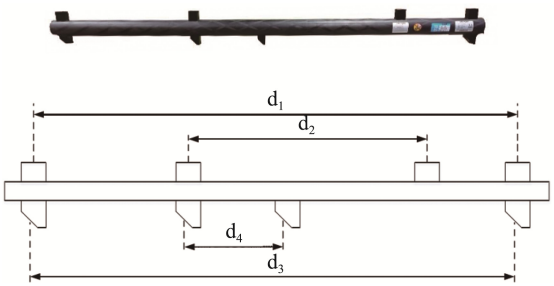

Fig.4 C-track Scale Bar

In the measuring range of the vision system, , the scale bar was measured. As shown in Fig.5, 25 different positions and poses of the scale bar of C-Track system were placed in space to make them cover the measuring range of the vision system as much as possible, and the length of d1, d2, d3 and d4 of the scale bar were computed

Table 2 Dimensions of C-track Scale Bar

	Reference Length/mm	Uncertainty/mm
d1	959.778	0.010
d2	479.386	0.009
d3	959.520	0.018
d4	160.186	0.016

Fig.5 C-track Scale Bar Length Measurement

The arithmetic measured mean of the 25 results, deviation and standard deviations of d1, d2, d3 and d4 were calculated and given in Table 3.

Table 3 Measurement data processing results

	Method	Mean/mm	Deviation/mm	SD/mm
d1	Zhang's Method	959.029	0.749	0.429
	Ref. [11]	959.289	0.489	0.153
	The Proposed Method	959.389	0.389	0.097
d2	Zhang's Method	479.600	0.214	0.190
	Ref. [11]	479.118	0.268	0.140
	The Proposed Method	479.453	0.067	0.117
d3	Zhang's Method	960.022	0.502	0.572
	Ref. [11]	959.930	0.410	0.256
	The Proposed Method	959.736	0.216	0.048
d4	Zhang's Method	160.142	0.044	0.173
	Ref. [11]	160.275	0.095	0.101
	The Proposed Method	160.204	0.018	0.044

According to the data shown in Table 3, the measurement accuracy and the repeatability of the proposed method proposed in this paper is are better than that of the two other methods, respectively.

7 Conclusion

In this paper, a method has been proposed to construct a virtual large reference plate with high-precision to calibrate a camera with large FOV. The experimental results show that we can improve the calibration accuracy in comparison with two existing methods, and the measurement accuracy and repeatability of a binocular vision system consitituted of two cameras calibrated with the proposed method can be improved significantly. As a future work, we will try to compensate the error of the guideway in order to improve the calibration accuracy further.

References

[1] Wu, C Q. (2022). Laser tracking attitude measurement based on improve visual orthogonal iterative method. *Chinese Journal of Scientific Instrument*, 43(7), pp. 63-71.

[2] Rout, A. (2022). Weld seam detection, finding, and setting of process parameters for varying weld gap by the utilization of laser and vision sensor in robotic arc welding. *IEEE Transactions on Industrial Electronics*, 69(1), pp. 622-632.

[3] Cong, M. (2019). Uncalibrated workpiece positioning method for peg-in-hole assembly using an industrial robot. *Instrumentation*, 004, pp. 26-36.

[4] Zhang, Z Y. (2000). A flexible new technique for camera calibration. *IEEE Transactions on Pattern Analysis and Machine Intelligence*, 22(11), pp.1330-1334.

[5] Liu, S G. (2014). Sub-regional camera calibration based on moving light target. *Optics and Precision Engineering*, 22(2), pp.259-265.

[6] Ye, N. (2017). A calibration trilogy of monocular vision based aircraft boresight system. *Measurement*, 117, pp.133-143.

[7] Yang, B. (2012). Camera calibration technique of wide-area vision measurement. *Acta Optica Sinica*, 32(9), pp.159-167.

[8] Yang, M. (2011). Accurate and Fast Field Calibration of Camera with Large FOV. *Electronics Optics and Control*, 18(6), pp.56-61.

[9] Sun, J H. (2009). Field calibration of stereo vision sensor with large FOV. *Optics and Precision Engineering*, 17(3),

pp.633-640.

[10] Zhang, X. (2017). High precision calibration of vision measurement system in large FOV based on virtual 3D target. *Optics and Precision Engineering*, 25(4), pp.891-899.

[11] Yu, L. (2018). A calibration method based on virtual large planar target for cameras with large FOV. *Optics and Lasers in Engineering*, 101, pp.67-77.

[12] Luhmann, T., Robson, S., Kyle, S., and Boehm, J. (2013). *Close-range photogrammetry and 3d imaging*. London: De Gruyter, pp.152-169.

Author Biographies

LIU Dong received the B.Sc. degree from Hefei University of Technology in 2020. He is now a M.Sc. candidate in Hefei University of Technology. His main research interest includes large-scale vision measurement.

E-mail: ldhfut@163.com

ZHANG Rui received the Ph.D. degree from Tianjin University, China, in 2017. He is now a lecturer in Hefei University of Technology. His main research interests include large-scale vision measurement, embedded system, etc.

E-mail: zhangrui@hfut.edu.cn

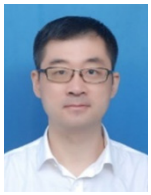

ZHANG Jin received the Ph.D. degree from Tianjin University, China, in 2010. He is now a professor and Ph.D. supervisor in Hefei University of Technology. His main research interests include vision measurement, dynamic test, etc.

E-mail: ldhfut@163.com

LI Weishi received the Ph.D. degree from Zhejiang University, China, in 2002. He is now a professor and Ph.D. supervisor in Hefei University of Technology. His main research interests include free-form surface inspection and reverse engineering, etc.

E-mail: weishili@hfut.edu.cn